Deep eutectic solvents as a stabilising medium for NAD coenzyme: unravelling the mechanism behind coenzyme stabilisation effect†

Mia Radović, [‡a] Lucija Hok, [‡b] Manuela Panić,[a] Marina Cvjetko Bubalo, [*a] Robert Vianello, [*b] Marijana Vinković[b] and Ivana Radojčić Redovniković[a]

Nicotinamide adenine dinucleotide (NAD) coenzyme is a vital part of numerous enzymatic reactions that are involved in all major biological processes from energy metabolism to cell survival. Accordingly, it is used in a great number of biocatalytic reactions, as analytical biosensors, and in test kits for diagnostic and analytical purposes. This coenzyme is unstable in aqueous solutions, meaning that the minimization of its degradation during storage, assays, and enzyme-catalysed oxidoreductive reactions is of high importance. Herein, we report on the stabilisation of NAD (NAD$^+$ as oxidised, and NADH as its reduced form) by deep eutectic solvents (DES), an emerging class of solvents that offer numerous remarkable advantages such as high tunability, and capability to stabilise a wide range of commercially important compounds of natural origin. Preliminary DES screening revealed that out of 7 candidates, choline chloride:urea (ChCl:U) shows the best ability to stabilise both NAD forms. Computational analysis (quantum chemical calculations and molecular dynamics simulations) provided a deeper insight into possible mechanisms behind the observed stabilisation, by identifying geometries and the solvation structure of NAD coenzymes in these solvents, and analysing their possible degradation pathways. Finally, prolonged NAD stability (up to 50 days) in ChCl:U is detected and the system is further confirmed as a stable working NAD solution in a model enzymatic assay.

Introduction

Over the past decade, deep eutectic solvents (DES) have emerged as a promising tool for shaping numerous processes into being more efficient and sustainable.[1] DES offer many remarkable advantages such as low volatility, non-flammability, low toxicity, and simple and solvent-free production from widely available natural raw materials. However, the most outstanding property of these solvents is their high tunability.[2,3] It is estimated that there are around 10^6 DES structural combinations. This exceptional structural flexibility provides the opportunity for rational solvent design to meet specific purposes and industrial requirements.[4]

The natural origin of DES allows these solvents to mimic the innate environment for various biomolecules and, to some extent, actively participate in the processes for which they are used.[5] In anhydrous form or as aqueous solutions, these solvents not only allow excellent solubility of various biomolecules *per se* but can also stabilise a wide range of commercially important natural compounds by favouring their particular molecular conformations.[6] For example, it has been demonstrated that DNA retains its structural integrity for at least 6 months when stored in a DES.[7] The stabilising effect of DES on various therapeutic proteins and industrial enzymes has also been confirmed in numerous studies.[8–13] As for the effect of DES on bioactive compounds, several research groups have observed that these solvents can fully meet the isolation, biological activity, and stability requirements of normally unstable polyphenolic compounds.[14–18] Finally, the improved solubility, stability, and bioavailability of various drugs (*e.g.* antibiotics and non-steroidal anti-inflammatory drugs) have also been successfully demonstrated by the introduction of therapeutic DES (THEDES) for oral and transdermal drug delivery.[19,20] However, these stabilisation effects are not yet fully understood and should be additionally investigated on a case-by-case basis using computational and experimental methods.

Nicotinamide adenine dinucleotide (NAD) coenzyme, the cell's hydrogen carrier, is an indispensable part of over 500 enzymatic reactions that regulate almost all major biological processes from energy metabolism to cell survival.[21] Despite

[a]University of Zagreb, Faculty of Food Technology and Biotechnology, Croatia. E-mail: mcvjetko@pbf.hr

[b]Ruđer Bošković Institute, Zagreb, Croatia. E-mail: robert.vianello@irb.hr

†Electronic supplementary information (ESI) available. See DOI: https://doi.org/10.1039/d2gc02656b

‡These authors contributed equally to this work.

its high cost, NAD is used in a great number of biocatalytic reactions, analytical biosensors, and test kits for diagnostic and analytical purposes.[22,23] Another limitation in the use of NAD coenzyme is its instability in the aqueous solution.[24] Therefore, to increase its stability toward hydrolysis (in acids and bases), great efforts have been made to develop synthetic NAD coenzymes that mimic the structure and function of natural molecules.[25] Another approach to minimize coenzyme degradation during storage, assays, and enzyme-catalysed oxidoreductive reactions, is stabilisation by a solvent. This has traditionally been achieved by selecting a buffer with an optimal pH value. However, when performing an enzyme-catalysed reaction, it is often very difficult to satisfy the pH requirements of all reaction participants, so typically pH value is adjusted to fit the enzyme used in the reaction.[26] Recently Zhang *et al.* found that by selecting neutral to basic ionic liquids and adjusting their concentration in the buffer, the NADH concentration can be maintained with little loss during CO_2 conversion catalysed by NADH-dependent formate dehydrogenase, resulting in improved conversion efficiency. This observation paves the way for improving the stabilisation of coenzymes by ionic liquids or other unconventional media as a neat, inexpensive, and green approach suitable for industrial application. Based on the above, the present work aimed to identify DES as NAD stabilisers. For this purpose, different betaine- and choline-based DES as stabilising media for NAD (NAD^+ as oxidised and NADH as reduced form) were investigated by UV-Vis spectroscopy. To decipher the mechanism behind the NAD stabilisation, molecular dynamics simulations and DFT calculations were performed. The prolonged stabilisation of

the coenzyme in DES (choline chloride:urea) at room temperature was tested as well as the biological functionality of the coenzyme (electron transfer in redox reactions) after incubation in DES by performing an alcohol dehydrogenase activity assay.

Experimental

Materials

Alcohol dehydrogenase from *Saccharomyces cerevisiae* (ADH) was purchased from Sigma-Aldrich, β-nicotinamide adenine dinucleotide hydrate (NAD^+) with 98% purity from Acros Organics, while β-nicotinamide adenine dinucleotide reduced disodium salt hydrate (NADH) with 97% purity was purchased from Alfa Aesar, Thermo Fisher Scientific. All DES components, namely betaine (B), choline chloride (ChCl), ethylene glycol (EG), propylene glycol (PG) were purchased from Thermo Fisher Scientific, except glycerol (Gly) from Lachner, and urea (U) from Gram-Mol. All before mentioned chemicals were commercial products of analytical grade and used without additional purification.

Solvent preparation

Preparation of betaine- and choline-based DES was performed by mixing hydrogen bond acceptor (HBA), hydrogen bond donor (HBD), and water in defined molar ratios (Tables 1 and 2).

Before use, choline chloride was dried in the vacuum concentrator at 60 °C for 24 h. The mixtures were stirred and heated up to 60 °C until a colourless and homogeneous liquid

---

Table 1 List of solvents used for NAD coenzyme stability screening

Deep eutectic solvents (DES)

| DES | DES components | | | Molar ratio of components | Abbreviation | Water content (wt%) | pH |
	1. HBA	2. HBD	3. Component				
Betaine-based DES	Betaine	Ethylene glycol	Water	1:2:4	$B:EG_4$	23	7.85
				1:2:8	$B:EG_8$	37	7.61
	Betaine	Glycerol	Water	1:2:4	$B:Gly_4$	19	7.86
				1:2:8	$B:Gly_8$	32	7.43
	Betaine	Propylene glycol	Water	1:2:4	$B:PG_4$	21	8.20
				1:2:8	$B:PG_8$	35	7.64
	Betaine	Urea	Water	$1:3:8^a$	$B:U_8$	33	6.20
Choline-based DES	Choline chloride	Ethylene glycol	Water	1:2:4	$ChCl:EG_4$	21	7.59
				1:2:8	$ChCl:EG_8$	35	7.42
	Choline chloride	Glycerol	Water	1:2:4	$ChCl:Gly_4$	18	4.33
				1:2:8	$ChCl:Gly_8$	30	4.74
	Choline chloride	Urea	Water	1:2:4	$ChCl:U_4$	21	10.14
				1:2:8	$ChCl:U_8$	35	9.94

Reference buffers

	Abbreviation	pH		Abbreviation	pH
NAD^+ reference buffers	PBS	7.00	NADH reference buffers	GlyPP	9.00
	Tris–HCl	7.00		Tris	9.50
	Water	7.15		Gly–NaOH	10.00

^{a} B:U at molar ratio 1:3:4 is a solid at room temperature.

Table 2 List of chosen ChCl:U solvents used for prolonged coenzyme stabilisation screening

DES components			Molar ratio	Water content (wt%)	Abbr.	pH
1	2	3				
Choline chloride	Urea	Water	1:2:2	10	ChCl:U$_{10\%}$	10.4
			1:2:4	20	ChCl:U$_{20\%}$	10.1
			1:2:6	30	ChCl:U$_{30\%}$	10.0
			1:2:14	50	ChCl:U$_{50\%}$	9.9
			1:2:22	60	ChCl:U$_{60\%}$	9.8
			1:2:48	80	ChCl:U$_{80\%}$	9.4

was formed. All prepared DES were stored in sealed bottles and later used for coenzymes stability and functionality experiments. The pH values of prepared DES were measured with a pH glass electrode (Mettler Toledo, Switzerland) and the obtained values are shown in Tables 1 and 2. Buffers were prepared according to standard protocols and their pH values were adjusted to fit in NAD$^+$ or NADH optimum pH range.

Monitoring NAD coenzyme stability

Preliminary measurements of NAD coenzyme stability in different solvents were monitored up to 14 days. NAD$^+$ and NADH (0.03 mg mL^{-1}) were separately incubated in 10 different solvents, namely 7 aqueous betaine- and choline-based DES and 3 reference buffers for each coenzyme (Table 1). Samples were kept in the dark at 25 °C and periodically measured on a UV-Vis spectrophotometer (Thermo Fisher Scientific, Genesys™ 10S) as follows: samples were poured in a quartz cuvette and absorption spectra from 230 to 400 nm were recorded for both NAD$^+$ and NADH solutions. Each measurement was carried out in triplicates. Absorption spectra of both coenzyme forms have a characteristic peak with an absorption maximum at 260 nm, due to the adenosine monophosphate unit. Additionally, only in the NADH absorption spectrum, a distinctive peak at 340 nm was observed.

This agrees with our excited-state TD-DFT calculations, which revealed that only NADH absorbs at 340 nm, being attributed to its neutral nicotinamide unit, which is absent upon its oxidation to the cationic form in NAD$^+$ (Fig. S1†).

The loss of absorbance at 340 nm or 260 nm for NADH and NAD$^+$, respectively, followed the first-order kinetics (1):

$$k_1 = \frac{2.303}{t} \log\left(\frac{A_0}{A_t}\right) \qquad (1)$$

where k_1 is the first-order rate constant (day^{-1}), A is the absorbance at 340 nm or 260 nm for NADH and NAD$^+$, respectively, either at time zero, A_0, or at time t, A_t.[27] After the initial screening (up to 14 days), the best DES candidate, namely ChCl:U, was chosen for a prolonged stabilisation observation (up to 50 days). The influence of different water shares was additionally investigated (Table 2).

For prolonged NAD$^+$ and NADH stability test, deviations of the absorbance values at 260 nm (Δ_{260}) and 340 nm (Δ_{340}), after 50 days of nicotinamide coenzyme incubation in relation

to the initial absorbance are calculated according to the eqn (2) and (3) and expressed as a percentage (%):

$$\Delta_{260} = \left|100 \times \frac{(A_{260'} - A_{260})}{A_{260}}\right| \qquad (2)$$

$$\Delta_{340} = \left|100 \times \frac{(A_{340'} - A_{340})}{A_{340}}\right| \qquad (3)$$

where $A_{260'}$ and $A_{340'}$ are the absorbances of the samples at 260 and 340 nm after the incubation, while A_{260} and A_{340} before the incubation of coenzyme in different solvents at 25 °C. For NADH, both Δ_{260} and Δ_{340} were calculated, while for NAD$^+$ just Δ_{260}. For NADH the A_{260}/A_{290} ratio, as an indicator of the coenzyme purity,[28] was calculated from the absorption spectra obtained prior and after 50-day incubation in DES and reference buffers.

Measurements of NAD coenzyme functionality

The functionality of the NAD$^+$ coenzyme was monitored through alcohol dehydrogenase (ADH) activity assay, on a UV-Vis spectrophotometer (Thermo Fisher Scientific, Genesys™ 10S), by a slightly modified method previously described by Vrsalović Presečki *et al.*, 2012.[29] Stock solutions of NAD$^+$ (0.05 g mL^{-1}) in ChCl:U$_{80\%}$ or Tris–HCl buffer were prepared and stored at +4 °C during 1, 2, 3, 4, 7 and 14 days. Before measurement in a quartz cuvette, NAD$^+$ (5 µL) was incubated for 10 minutes at room temperature in GlyPP buffer (975 µL). The reaction was initiated by the addition of ethanol (96%, v/v, 10 µL) and freshly prepared ADH (0.4 mg mL^{-1}, 10 µL). The reduction rate of NAD$^+$ was immediately monitored for 3 minutes at a fixed wavelength of 340 nm. The ADH activity was calculated from changes in absorbance at 340 nm through time. The reaction was measured in triplicates. Volumetric ADH activity (A_v, µmol cm^{-3} min^{-1}) was calculated according to the expression (4):

$$A_v = \frac{\Delta A}{\Delta t} \cdot \frac{V_t}{V_s \cdot \varepsilon_{340} \cdot d} \qquad (4)$$

where, $\Delta A/\Delta t$ is the absorbance change in time (min^{-1}); V_t is total volume (cm^3); V_s is sample volume (cm^3); ε_{340} is extinction coefficient (6.22 cm^2 µmol^{-1} for NADH at $\lambda = 340$ nm); d is cuvette diameter (cm).

Computational details

Quantum-chemical calculations. All structures were optimized by a very efficient DFT M06-2X/6-31+G(d) model employing the implicit SMD solvation with all parameters for pure water. Thermal corrections were extracted from the corresponding frequency calculations so that all presented results correspond to Gibbs free energies at room temperature and normal pressure. The choice of such computational setup was prompted by its success in reproducing various features of different organic,[30,31] organometallic,[32] and protein systems,[33–35] being particularly accurate for relative trends among similar systems, which is the focus here. In addition, the validity of the SMD implicit model in evaluating solvation

effects on the reactivity parameters has recently been emphasized by various groups.[36–38] All transition state structures were located with the help of the scan procedure, employing both 1D and 2D scans, the latter specifically utilized to exclude the possibility for concerted mechanisms, and then fully optimized as saddle points on the potential energy surface. Apart from the visualization of the obtained negative frequencies, the validity of all transition states was confirmed through IRC calculations in both directions. Excited state calculations were performed at the same level of theory employing the TD-DFT approach considering 32 lowest singlet electronic excitations. All the calculations were conducted with the Gaussian 16 software.[39]

Molecular dynamics simulations. To parameterize both coenzymes and all DES components, their RESP atomic charges were calculated at the HF/6-31G(d) level of theory. In order to match our simulations with experimental conditions, for DES solutions the precise number of 200 choline molecules, 400 glycerol/urea molecules, and 800 waters was placed around each coenzyme with the PackMol utility. For simulations in pure water, each coenzyme was solvated in a truncated octahedral box of TIP3P waters spanning a 10 Å-thick buffer. Both coenzymes were considered in their physiological protonation forms, NAD^+ as a monoanion, and NADH as a dianion, so the matching simulation boxes were neutralized with one and two Na^+ ions, respectively, while the simulations including choline were supplemented with the equal number of Cl^- anions. The obtained complexes were submitted to the geometry optimization in Amber 16,[40] employing periodic boundary conditions in all directions. In all instances, optimized systems were gradually heated from 0 to 300 K and equilibrated during 30 ps using *NVT* conditions, followed by a productive and unconstrained MD simulation for 300 ns, employing a time step of 2 fs at constant pressure (1 atm) and temperature (300 K), the latter held constant using a Berendsen barostat and a Langevin thermostat with a collision frequency of 1 ps^{-1}. The long-range electrostatic interactions were calculated employing the particle mesh Ewald method[41] and were updated in every second step, while the nonbonded interactions were truncated at 11.0 Å, all in line with our earlier reports on similar systems.[33,34]

QM/MM ONIOM calculations. In order to verify the accuracy of mechanistic DFT calculations, we have repeated the analysis for a selected number of cases with the hybrid QM/MM ONIOM approach, where the input structures were obtained through the clustering analysis of the corresponding MD trajectories using the DBSCAN utility implemented in Amber 16.[42] All geometries were optimized by the M06-2X/6-31+G(d): AMBER model with the electrostatic embedding as implemented in Gaussian 16, since a similar approach was used by Wetmore and co-workers to model DNA nucleobases.[43,44] To avoid the impact of artificially created interactions among solvent molecules on the total energy as a result of a contact with vacuum, the outer part of the MM region was kept fixed during optimization as recommended in the literature.[45] In all calculations, the entire coenzyme geometry, with the addition of one reactive $H_2O/H_3O^+/OH^-$ molecule for the P–O hydrolysis, was included in the QM region, while the rest of the environment was treated within the MM region.

Results and discussion

Pursuing to minimize degradation of NAD coenzyme during storage, reagent preparation, and assays, we investigated the potential of DES to stabilise the NAD coenzyme (oxidized and reduced form). For that purpose, changes in NAD UV-Vis absorption spectra during the 14-day incubation period in different betaine- and choline-based DES at room temperature were monitored. To better understand the experimental data and reveal the mechanisms underlying the DES stabilisation effect, a computational approach was implemented using molecular dynamics (MD) simulations and quantum mechanics (QM) calculations. DES that exhibited the highest stabilisation potential for both coenzyme forms were further used in the prolonged coenzyme stabilisation and activity studies by using the alcohol dehydrogenase (ADH) activity assay.

Screening of the NAD coenzyme stability in DES

The DES selection is the first and crucial step in finding the right fit for a specific purpose. To meet the requirements of green chemistry, DES selected for the screening of the NAD coenzyme stability were prepared from cheap, readily available, biodegradable, and biocompatible components.[46] Additionally, chosen choline chloride- and betaine-based DES with amide urea or polyols have been shown as promising media for stabilisation of various biomacromolecules such as DNA, plant and microbial secondary metabolites, and proteins.[6] Furthermore, since it has been shown that DES-assisted stabilisation of macromolecules is not primarily governed by DES acidity/basicity, which is determined by the acidity/basicity constants of HBD and HBA used and their combination, but rather occurs through the establishment of multi-level and specific interactions such as electrostatic attraction, hydrophobic and polar interactions.[6] Thus, DES used in this study were chosen regardless of their pH (in the range from 4.33 to 10.44) and were used without post preparation modifications. Finally, as the NAD coenzyme is an indispensable part of diverse enzyme-catalysed reactions, considered DES have been shown as effective in activating and stabilising various types of enzymes.[5]

Betaine- and choline-based DES containing amide (urea) or polyol (ethylene glycol, glycerol, or propylene glycol) as hydrogen bond donors at two HBA-to-water molar ratios of 1:4 or 1:8 (corresponding to 18–37 wt% of water in DES–water mixture) (Table 1) were firstly screened as NAD stabilising medium by observing changes in the coenzyme UV-Vis absorption spectrum (230–400 nm) during 14 days at room temperature. At these water contents (<40 wt%) it is presumed that hydrogen bond network is maintained (DES inherent property), while the addition of water above this value would result in a solution that exhibits behaviour closer to that of solutes in an aqueous solution.[47] Additionally, at the water contents used

in this study, the eutectic systems are expected to possess properties beyond the sum of their parts (components). As reference solvents, buffers with optimal pH value for each coenzyme form were considered (pH = 6–7 for NAD$^+$ and pH = 9–10 for NADH). During the incubation time the loss of absorbance at 260 nm (corresponding to degradation changes in adenine group),[28,48] and 340 nm (corresponding to changes in nicotinamide unit)[49] for NAD$^+$ and NADH, respectively, followed first-order kinetics.[27] Degradation rate constants observed during coenzymes' incubation in DES and reference buffers are presented in Fig. 1. From the obtained results it is obvious that DES composition plays a significant role in the coenzyme degradation rate. In general, betaine-based DES were less suitable for stabilisation of both coenzyme forms than choline-based DES. This is particularly pronounced for NADH in DES with EG as a HBD (e.g. in ChCl:EG$_4$ the calculated degradation constant is k_{NADH} = 0.0061 day^{-1}, while in B:EG$_4$ the corresponding constant is k_{NADH} = 0.0261 day^{-1}). When comparing the influence of HBD on NAD degradation rate, it can be concluded that glycerol shows a stronger destabilising effect on NAD coenzyme compared to other HBDs. For example, NADH is degraded almost 5-fold faster in ChCl:Gly than in ChCl:U. In general, HBA-to-water molar ratio did not significantly affect DES stabilising properties. Only for betaine-based DES with ethylene glycol and glycerol as HBD lower water contents beneficially influenced DES ability to stabilise the coenzyme. This is the most pronounced for B:Gly where degradation constants for B:Gly$_4$ and B:Gly$_8$ are k_{NADH} = 0.0398 day^{-1} and k_{NADH} = 0.1056 day^{-1}, respectively.

The preliminary screening revealed that out of 7 DES candidates, ChCl:U shows the best stabilisation potential for both coenzyme forms (k_{NADH} = 0.0052–0.0056 day^{-1} and k_{NAD^+} = 0.0042–0.0048 day^{-1}), followed by ChCl:EG (k_{NADH} = 0.0061–0.0062 day^{-1} and k_{NAD^+} = 0.0061–0.0069 day^{-1}). Additionally, when comparing the results obtained in ChCl:U and ChCl:EG with the results obtained in the best reference buffers (k_{NADH} = 0.0081 day^{-1} for NAD$^+$ in Tris–HCl (pH = 7); k_{NADH} = 0.0071 day^{-1} for NADH in Tris (pH = 9.5)), a significant improvement in NAD coenzyme stability in the DES is observed, which for NADH and NAD$^+$, assumes 20 and 50%, respectively. The screening result is quite extraordinary since the coenzyme's two forms prefer a medium with different pH values: NAD$^+$ being more stable in a neutral to a slightly acidic environment (pH$_{optimum}$ = 6–7), and NADH in a basic environment (pH$_{optimum}$ = 9–10).[27] Yet ChCl:U (pH ≈ 10) stabilises both coenzyme forms while it should be expected to stabilise only NADH. The same is observed for ChCl:EG with pH value close to optimal for stabilisation of NAD$^+$ (pH ≈ 7.5), but is still equally efficient in stabilising NADH. These results strongly imply pH-independent behaviour of the coenzyme in these DES. Thus, to get insight into the ChCl:U ability to stabilise both NAD forms and possible NAD degradation pathways, a detailed computational analysis was performed.

Computational analysis of DES stabilisation effect

Computational analysis was performed to identify relevant intermolecular interactions with coenzymes in solution and evaluate their significance for degradation processes leading to their instabilities. Our DES screening (Fig. 1) showed the superiority of choline-based DES over betaine-based analogues, while also proving the significance of the right HBD fit. It seems that glycerol (Gly) provides a minimal, while urea (U) the largest contribution to the NAD stabilisation. Thus, in our computations, we considered pure water as a reference system and two choline-based DES, ChCl:Gly and ChCl:U. Although the literature advises on several NAD$^+$/NADH degradation pathways, including the nucleophilic addition to the pyridine ring,[24] here we focused on (i) the cleavage of the nicotinamide–ribosyl bond, and (ii) the hydrolysis of the phosphodiester P–O bond, as dominant sources of instabilities. Specifically, the nucleophilic addition to pyridine is preceded by a general acid-catalysed protonation at C-5,[24] for which highly acidic conditions are required,[50] much beyond those experimentally employed here. Instead, the cleavage of the nicotinamide–ribosyl bond occurs under neutral and especially elevated basic conditions and is initiated by the ionization of the ribose diol (pK_a = 11.9).[51] Lastly, the phosphodiester hydrolysis can also take place under conditions close to neutrality, yet it will be particularly favoured as acid- or base-catalysed processes.[52,53]

Conformational aspects of coenzymes in solution

We first inspected the conformational flexibility of coenzymes to elucidate representative geometries in all three considered environments. In all MD simulations, each coenzyme was initially inserted into the simulation box in a fully extended conformation. Yet, in pure water, these quickly folded into
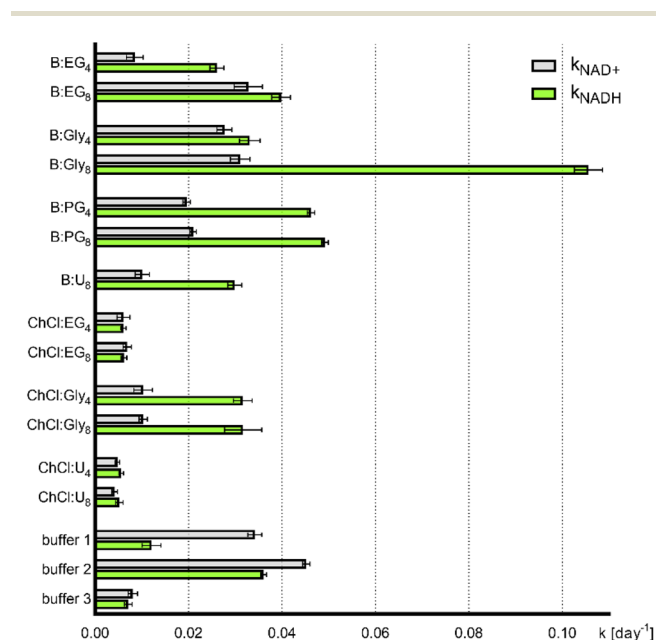
Fig. 1 Degradation constants during NAD$^+$ and NADH incubation in DES and reference buffers. Buffer 1: PBS (for NAD$^+$) and Gly–NaOH (for NADH); buffer 2: water (for NAD$^+$) and GlyPP (for NADH); buffer 3: Tris–HCl (for NAD$^+$) and Tris (for NADH).

bent structures in both cases, and predominantly remained as such (Fig. 2). This is brought about through favourable hydrophobic π···π stacking interactions between pyridine and adenine aromatic rings, whose centres of mass are found below 5 Å during 66% and 62% of the simulation times, respectively (Fig. S2†). This is in line with our DFT calculations which showed that bent conformations are by 5.5 and 2.8 kcal mol^{-1} more stable than matching extended analogues in NAD$^+$ and NADH, thus further confirming the validity of MD simulations. As seen in Fig. 2, in pure water, both phosphates in each NAD form are not participating in any intramolecular interactions with the rest of the molecule. This leaves them exposed to the solvent, as evidenced in the fact that each of the phosphate O-atoms forms as much as three hydrogen bonding contacts with the surrounding waters in the first solvation shell (Fig. S3 and Tables S1, S2†). The latter makes this part of the molecule sensitive towards hydrolysis and defines its tendency to undergo the water-assisted P–O cleavage; an issue that we will come back to later in the text. The same is observed for both ribose units and their hydroxyl groups, whose interactions with the surrounding solvent, and the resulting acidity is basically not hindered in any way.

A change in the environment is immediately reflected in geometrical preferences for NAD$^+$ and NADH. This is relatively moderately seen in ChCl:Gly (Fig. S4†), where both coenzymes abandon their hydrophobic π···π stacking contacts, and switch to more extended conformations as dominant. However, this again occurs without any intramolecular hydrogen bonding contacts. In contrast, when ChCl:U is considered (Fig. S5†), both coenzymes again reveal a complete lack of the π···π stacking interactions, yet over 90% of the obtained structures for NAD$^+$ are characterized with the intramolecular hydrogen bonding among nicotinamide amide and either one of the phosphate units or the –OH group from ribose attached to adenine. The former are more relevant, as such persistent N–H···O$^-$ interactions could likely contribute towards increased stability of NAD$^+$ in ChCl:U relative to ChCl:Gly with respect to the phosphodiester hydrolysis. In other words, the mentioned interaction reduces the negative charge on the phosphate making it less susceptible towards hydrolytic cleavage.
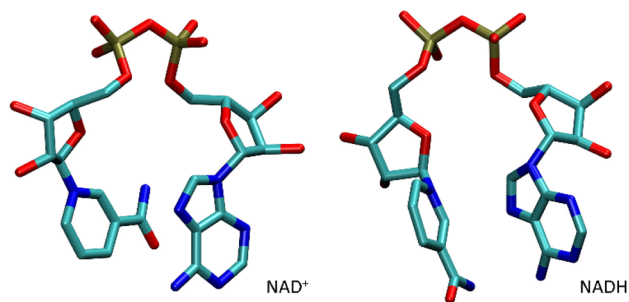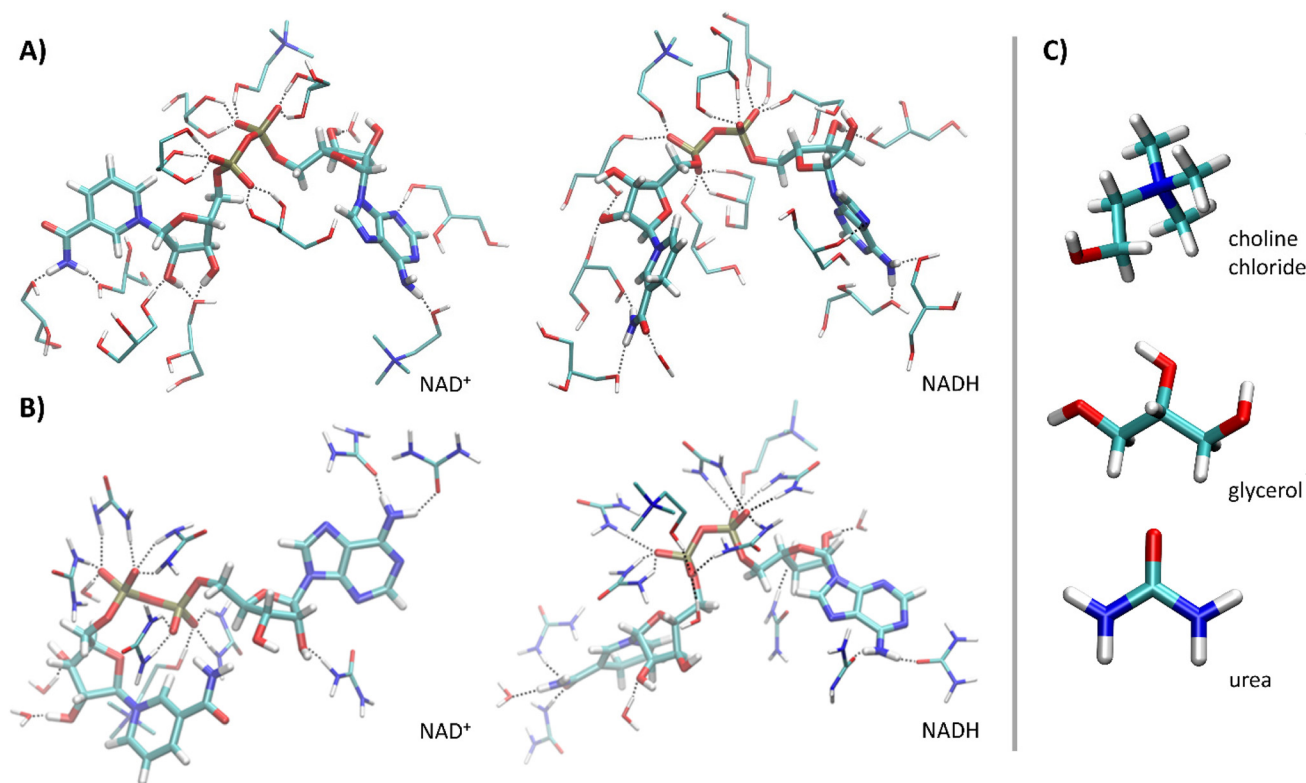
In finishing this section, let us reiterate that, in pure water, the geometry of coenzymes is dominated by the tendency to undergo the hydrophobic π···π stacking interactions between pyridine and adenine rings that allow bent structures without any intramolecular hydrogen bonds. When DES components are introduced, the resulting environment disfavours any pairing between aromatic rings and offers more extended conformations, which in ChCl:U further leads to the intramolecular hydrogen bonding involving phosphate unit and nicotinamide. Both aspects possibly influence the coenzyme stability in DES, especially in ChCl:U, which is experimentally determined as the most promising media in this respect.

Cleavage of the phosphodiester P–O bond

As mentioned, phosphodiester groups in both NAD coenzymes are generally not participating in intramolecular interactions and are significantly exposed to the solvent, especially in pure water. To further confirm that, the actual number of hydrogen bonds that each coenzyme fragment makes with solvent waters (Table S3†) indicates that phosphodiester units are accounting for as much as around 54% of the total number of such contacts in NAD$^+$ and 52% in NADH. At the same time, phosphates are between 4–5 times more frequent in this respect than any of the remaining fragments. This is not surprising knowing that each phosphate bears a negative charge which makes it attractive for water solvation. On the other hand, nicotinamide in NAD$^+$ is less prone to hydrogen bonds with solvent than its analogue in NADH despite bearing the charged pyridine unit. This only confirms that the excess positive charge in NAD$^+$ is resonantly dispersed around the entire nicotinamide, which diminished its effect on the solvation (Fig. S6†). Lastly, although the total number of hydrogen bonds is around 7% higher in NADH, the particular portion ascribed to phosphates is practically identical for both coenzymes, therefore not contributing towards differences in the coenzyme stability in the aqueous solution.

Once pure water is replaced with DES, the solvation of both NAD coenzymes is reduced, as seen in a lower total number of hydrogen bonds in both cases. This is found between 20% and 30%, depending on DES and the coenzyme. What is particularly relevant is that in ChCl:Gly, the solvation of phosphates is drastically changed in a way that the number of hydrogen bonds with waters is significantly reduced, by 95% in NADH and by 97% in NAD$^+$. Such a dramatic change in the solvation is brought about by DES components that overtake the role of solvating phosphates from waters. With both coenzymes, choline is much less efficient in this, while glycerol clearly dominates in this respect. Specifically, in ChCl:Gly, glycerol molecules account for around 89% of hydrogen bonding contacts with phosphates in NAD$^+$ and around 90% in NADH. This is significant and leads us to conclude that in ChCl:Gly the first solvation sphere around phosphates in both coenzymes is almost exclusively composed of glycerol molecules (Fig. 3A and Tables S1–S3†). Accordingly, when ChCl:U is employed, the same trend is observed (Fig. 3B and Tables S1–S3†). There, the number of hydrogen bonds with waters is

Fig. 2 Representative structures of NAD$^+$ and NADH in water, which account for 89% and 86% of all structures during MD simulations. Hydrogen atoms are omitted due to clarity.

Fig. 3 Representative structures of NAD coenzymes in (A) ChCl:Gly, and (B) ChCl:U system during MD simulations indicating the predominance of glycerol or urea, respectively, in solvating both NAD coenzymes. (C) Enlarged structures of DES components.

reduced by 89% in NAD$^+$ and by 86% in NADH relative to the pure aqueous solution, and this role is predominantly taken by urea molecules, which turn out as most efficient in solvating anionic phosphates. Specifically, ureas form N–H⋯O hydrogen bonds with phosphates that account for 77% of the total hydrogen bonds in NAD$^+$ and 66% in NADH.

All these results point to several conclusions. In pure water, phosphates are very efficiently solvated by waters and this fact defines the sensitivity of P–O bonds towards the hydrolytic cleavage. Once DES are introduced, their components turn out as more efficient in solvating phosphates than waters themselves. This clearly diminishes the ability of water molecules to approach these anionic fragments and undertake the hydrolytic reaction. As such, this provides a convincing reason why both of the studied DES solutions provide some coenzymes stability relative to pure water. However, in order to precisely interpret relative differences among DES solutions, we need to inspect the nucleophilicity of DES components, as choline, glycerol, and urea can, on their own, undertake solvolytic cleavage of the P–O bonds. For that purpose, we performed several DFT calculations for the model reaction, considering all the mentioned possibilities (Table 3).

Phosphoric acid diesters are, in general, exceedingly unreactive in water, which is, among other things, relevant for sustaining life on Earth, since this feature allows the phosphodiester linkages that join DNA nucleotides to be highly resistant to spontaneous hydrolysis. For example, the uncatalysed

Table 3 Calculated activation ($\Delta G^{\ddagger}$) and reaction (ΔG_R) free energies for the cleavage of the P–O bond in model phosphodiester induced by different nucleophiles in water. All values are in kcal mol^{-1} and are obtained through the (SMD)/M06-2X/6-31+G(d). Relevant experimental data are placed within squared brackets for comparison

Nucleophile (X)	$\Delta G^{\ddagger}$	ΔG_R
H$_2$O	44.7 [44.3]$_{EXP}$[54]	−0.6
OH$^-$	25.1 [25.9]$_{EXP}$[55]	−18.9
H$_3$O$^+$	17.4 [16.9]$_{EXP}$[56]	−17.1
Glycerol (Gly)	42.4	−0.9
Urea (U)	38.5	21.7
Choline (Ch)	44.3	−2.0

hydrolysis of dimethyl phosphate in neutral solution was found to proceed with an estimated rate constant of ≈2 × 10^{-13} s^{-1} at 25 °C, corresponding to a half-time of 140 000 years.[57] Our calculations firmly support such a notion through a very high activation barrier of 44.7 kcal mol^{-1} and only a moderate exergonicity of −0.6 kcal mol^{-1}, which jointly suggest a fairly unfavourable reaction and a very slow process. The former agrees with the value obtained by the ONIOM approach, 45.7 kcal mol^{-1}, while both are found in line with the barrier of 44.3 kcal mol^{-1} experimentally determined for phosphomo-

noester dianions in aqueous solution,[54] which confirms the validity of computed results. Once we move from the solution neutrality, this reaction becomes exceedingly feasible. In alkaline media, OH⁻ anions are more nucleophilic than water, and their approach towards the P–O bond reduces the activation barrier to 25.1 kcal mol⁻¹ (20.5 kcal mol⁻¹ with ONIOM), found in excellent agreement with 25.9 kcal mol⁻¹ measured by Zalatan and Herschlag,[55] and increases the reaction free energy to −18.9 kcal mol⁻¹, thereby indicating a favourable process. Moreover, the reaction in acidic media is even more likely, as the kinetic barrier is further reduced to 17.4 kcal mol⁻¹ (19.9 kcal mol⁻¹ in the ONIOM approach), which also agrees with the experimental value of 16.9 kcal mol⁻¹ for the analogous guanidinium-promoted nucleophilic mechanism.[56] All of this strongly indicates that the stability of coenzymes, with the respect to the P–O cleavage, will be highest at the solution conditions close to neutrality. Yet, what is even more relevant is the fact that both glycerol and choline share around the same nucleophilicity as waters, which precisely justifies why ChCl:Gly does not provide significant stabilisation to either coenzyme. In contrast, in ChCl:U, our earlier results showed that urea dominates in solvating anionic phosphates (Fig. 3B), yet its nucleophilicity is drastically lower than for water. Specifically, urea allows a 6.2 kcal mol⁻¹ reduction in the kinetic barrier relative to water, yet the reaction becomes significantly endergonic (ΔG_R = 21.7 kcal mol⁻¹), which makes this reaction highly unfeasible. This goes on top of the fact that urea solvates phosphates through amide N–H bonds, while the solvolytic cleavage of the P–O bond can only occur through the matching O-atom in urea. Therefore, we can conclude that the observed stabilising effect of ChCl:U originates in the fact that introduced urea molecules predominate in solvating phosphates, which, on one hand, prevents water molecules from approaching and cleaving P–O groups, while urea does not possess enough nucleophilicity to initiate the coenzyme degradation on its own.
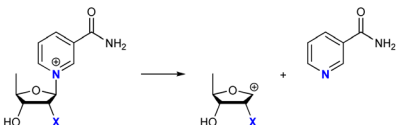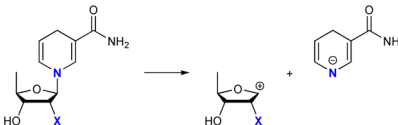
Lastly, we note in passing that we observed an additional small stabilising effect in ChCl:U for NAD⁺. Namely, this environment allows such NAD⁺ conformations, which favour intramolecular hydrogen bonding between nicotinamide amide and its nearest phosphate unit (Fig. 3), which is persistent during 88% of the simulation time (Fig. S7†) and occurs at the average N–H⋯O distance of 2.89 Å.

Cleavage of the nicotinamide–ribosyl N–C bond

NAD⁺ has long been known to be unstable toward basic conditions, undergoing specific base-catalysed cleavage of the nicotinamide–ribosyl N–C bond.[51] Johnson and co-workers found that the pH profile for the hydrolysis of NAD⁺ paralleled the ionization of the ribose diol (pK_a = 11.9) establishing that the strongly electron-donating diol anion was responsible for the alkaline lability of NAD⁺.[59] Our DFT calculations confirm these observations, as when the ribose unit is unionized (Table 4, X = OH), the cleavage of the N–C bond is highly unfeasible in both coenzymes. Specifically, in neither coenzyme we were not able to locate the matching transition state for this process, while the obtained reaction free energies are exceedingly endergonic, 23.7 kcal mol⁻¹ for NAD⁺ and as much as 48.8 kcal mol⁻¹ for NADH, which make the examined processes very unlikely under normal conditions. Yet, upon increasing solution pH conditions, the reactions start to become more feasible, which in NADH is evidenced only in the improved reaction free energy to 19.9 kcal mol⁻¹, still being highly endergonic, thus unfavourable. This goes in line with a very high kinetic barrier of 43.2 kcal mol⁻¹, which jointly suggests practically no NADH vulnerability towards breaking the nicotinamide–ribosyl bond, even at increased pH conditions. In contrast, the situation with NAD⁺ is different, as instantly when the solution conditions allow the ribose –OH deprotonation, the cleavage of the N–C bond proceeds through a modest kinetic barrier of $\Delta G^{\ddagger}$ = 18.4 kcal mol⁻¹ (19.4 kcal mol⁻¹ with the ONIOM method) and liberates ΔG_R = −10.7 kcal mol⁻¹ of the reaction free energy. We again emphasize the accuracy of our computational setup as the calculated barrier ties in with 19.7 kcal mol⁻¹ determined experimentally at pH = 7.4,[58] while the computed reaction exergonicity agrees with the experimental value of ΔG_R = −8.2 kcal mol⁻¹ reported by Rising and Schramm.[60] Even under neutral conditions, this

Table 4 Calculated activation ($\Delta G^{\ddagger}$) and reaction (ΔG_R) free energies for the cleavage of the nicotinamide–ribosyl N–C bond under different circumstances. All values are in kcal mol⁻¹ and are obtained through the (SMD)/M06-2X/6-31+G(d) calculations. Relevant experimental data are placed within squared brackets for comparison

NAD coenzyme	Degradation reaction	X = OH		X = O⁻	
		$\Delta G^{\ddagger}$	ΔG_R	$\Delta G^{\ddagger}$	ΔG_R
NAD⁺		—	23.7	18.4 [19.7]$_{EXP}$[58]	−10.7
NADH		—	48.4	43.2	19.9

process will have a significant progress, since, at pH = 7, it requires only 6.7 kcal mol^{-1} to deprotonate a diol with pK_a = 11.9, which is lower than the entire reaction free energy (ΔG_R = −10.7 kcal mol^{-1}), thus is feasible. This notion helps explaining two experimental observations; given a high sensitivity of NAD$^+$ towards the N–C cleavage, it is reasonable that (i) the optimal pH for NAD$^+$ is in the acidic region (pH = 6–7), while NADH can tolerate slightly alkaline media (pH = 9–10), and (ii) the initial stability of NAD$^+$ is much lower relative to NADH, seen here in all three employed buffers, and assuring its long-term stability poses a bigger challenge. Because of that, the subsequent analysis will mostly focus on NAD$^+$, but some aspects relative to NADH will also be discussed.

In order to interpret the effect of DES solutions on these processes, we again rely on the number of hydrogen bonding contacts that solution components are making with the matching nicotinamide ribose unit (Table S3†), but also look more specifically towards the relevant –OH group as a hydrogen bond donor (Table S4†), which follows the same trend and which evaluates its ability to undergo deprotonation and, subsequently, degradation. In pure water, the mentioned total number pertaining to the nicotinamide ribose is slightly higher for NADH, but for both coenzymes, it is around 300 000. Given that our analysis is based on 150 000 structures in final MD trajectories, this implies that, on average, each of the two hydroxyl –OH groups in both coenzymes forms a persistent hydrogen bonding with one water molecule during the entire simulation time. Such a situation serves as a reference for its tendency to initiate the N–C bond cleavage.

In ChCl:Gly, the number of ribose diol–water contacts in NAD$^+$ is reduced by 85% relative to the pure aqueous solution, while 68% in ChCl:U, which already hints at an increased stability of NAD$^+$ in these media. Moreover, although water molecules in these interactions are replaced by DES components, the total number of hydrogen bonding contacts that nicotinamide diols in NAD$^+$ are experiencing is reduced by 46% in ChCl:Gly and by 36% in ChCl:U, which further confirm the stabilising influence of DES. We notice that both effects are more pronounced in ChCl:Gly, which would indicate its dominance over ChCl:U. However, to precisely interpret the relative trend among DES solutions, we note that the ability of nicotinamide diol to undergo deprotonation depends on the basicity and the proton-accepting capacity of the surrounding media. In this respect, we note that in ChCl:Gly the nicotinamide ribose is predominantly solvated by glycerol, around three times more often than with water. Still, glycerol is less basic (pK_a = −3.0) than water (pK_a = −1.75), thereby confirming the generally lower basicity of aliphatic alcohols over water.[61] This suggests a somewhat hindered diol deprotonation and a moderate NAD$^+$ stabilisation effect. On the other hand, in ChCl:U, the solvation of the nicotinamide ribose is exchanged between water and urea, where the latter is further less basic (pK_a = −3.9).[62]

This, in line with its previously demonstrated poor O-nucleophilicity, additionally disfavours the diol deprotonation, thus provides extra stabilisation. Lastly, we note that the

ability of choline to approach nicotinamide diols in NAD$^+$ is very poor (Table S3†), while its basicity (pK_a = −3.2) is close to that of glycerol, therefore its influence on the examined processes is negligible. In conclusion, we can underline that the cleavage of the nicotinamide–ribosyl N–C is an even more feasible process than the phosphodiester hydrolysis, yet only for NAD$^+$, and only once its nicotinamide ribose diol is deprotonated. Both DES systems reduce the overall solvation of the mentioned diol, which disfavours its deprotonation and contributes towards the NAD$^+$ stability, while DES components, glycerol in ChCl:Gly and urea in ChCl:U additionally compete with waters for solvent–diol hydrogen bonding contacts. Given that glycerol is less basic than water, while urea even further, rationalizes a better stabilisation effect of ChCl:U over ChCl:Gly.

In finishing this section, let us briefly mention that the cleavage of the analogous adenine–ribosyl N–C bond is much less favourable than for the described nicotinamide–ribosyl case (Tables S5 and S6†). Specifically, while for neutral ribose the reaction is highly endergonic (ΔG_R = 36.6 kcal mol^{-1}), even the diol deprotonation does not facilitate this process. Specifically, the calculated activation barrier is by 11.1 kcal mol^{-1} higher at $\Delta G^{\ddagger}$ = 29.5 kcal mol^{-1}, while the overall reaction is even endergonic at ΔG_R = 4.8 kcal mol^{-1}. Both aspects jointly suggest the unfeasibility of this degradation process, and we did not consider it any further.

Prolonged NAD coenzyme stability in ChCl:U

The preliminary solvent screening and additional computational analysis confirmed ChCl:U as the best candidate for the NAD coenzyme stabilisation. Thus, ChCl:U was chosen for further validation of DES as an alternative medium for long-term NAD coenzyme storage (*e.g.* as a working reagent solution). Additionally, to get better insight into the influence of DES water content on coenzyme stabilisation, ChCl:U with 6 different water shares, in the range from 10 to 80% (w/w), was evaluated and compared to optimal buffer solutions (Tris–HCl for NAD$^+$ and Tris for NADH) (Table 2). As during preliminary DES screening, changes in absorption maximums at 260 and 340 nm during NAD incubation up to 50 days were monitored. To get a clearer insight into the deformation of NAD spectra during incubation in ChCl:U and reference buffers, changes were expressed as deviations in absorption maximums in regards to initial absorption values (%). For NADH additional spectral change at 290 nm was monitored as this also allows one to assess the purity of the NADH solution.[28]

We observed that the increase of water content causes the increase of Δ_{340}, therefore negatively affects the NADH stabilisation (Fig. 4). On the other hand, no clear correlation between DES–water content and Δ_{260} of both NADH and NAD$^+$ was noticed. That could imply that water strongly destabilises only the dihydropyridine ring of NADH but has no influence on adenosine monophosphate in both coenzyme forms, in line with computational analysis that identified the former structural unit as more susceptible towards degradation. The most favourable solvent for NAD$^+$ stabilisation was ChCl:U$_{80\%}$ with the lowest absorption deviation (Δ_{260} = 6.17%) while for NADH
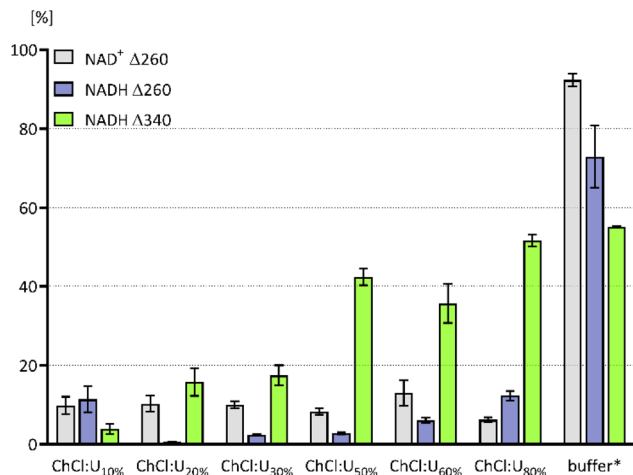
Fig. 4 Deviations (%) in the absorption maximums of NAD$^+$ (at 260 nm) and NADH (at 260 and 340 nm) after 50-day incubation in ChCl:U with 6 different water shares and reference buffers. *Buffer: Tris–HCl for NAD$^+$ and Tris for NADH.

it was ChCl:U$_{10\%}$ (Δ_{260} = 11.35% and Δ_{340} = 3.89%). Further, both reference buffers cause significantly higher absorption deviations than any tested DES, meaning that they are not suitable for prolonged coenzyme incubations. Considering the overall results, ChCl:U$_{10\%}$ provides the best results simultaneously for both NAD coenzyme forms, and is further considered as a potential sole incubation media.

Fig. 5 illustrates prolonged NAD stabilisation by comparing whole absorption spectra before coenzyme incubation and

after 21 and 50 days in the best DES (ChCl:U$_{10\%}$) and reference buffer. While the NAD coenzyme absorption spectra of both forms retain almost the same shape after a 50-day incubation period in ChCl:U$_{10\%}$, it is obvious that is not the case in reference buffers, proving DES superiority in coenzyme stabilisation. Also, analysing NADH absorption spectra at 290 nm, it can be seen that no significant changes were detected after 50 days of incubation in ChCl:U$_{10\%}$ (Fig. 5D). Meanwhile, a drastic absorption spectrum deformation in Tris buffer can be seen in Fig. 5C. The observed increase in absorbance at 290 nm during NADH incubation is related to acid-degradation products and gives a clear insight into the deteriorating NADH purity.[28]

To additionally confirm ChCl:U$_{10\%}$ stabilisation effect on NADH the A_{260}/A_{290} ratios, as an indicator of the coenzyme degradation,[28] before and after the 50-day incubation were calculated. In ChCl:U$_{10\%}$ the A_{260}/A_{290} ratio prior and after incubation was excellently preserved (10.3 and 10.9, respectively), while in the reference buffer (TRIS) a decrease in the ratio of 94% was observed (10.9 and 0.7, respectively). Therefore, it is safe to say that the results imply excellent NADH stability in ChCl:U$_{10\%}$ relative to the reference buffer.

Another important observation when conducting the prolonged NAD stability test is that no contamination was found in any DES sample during a 50-day incubation period. On the other hand, turbidity was frequently developed in buffer-coenzyme solutions, in some cases resulting in contamination. This important observation leads us to conclude that solutions of NAD coenzyme in ChCl:U are less susceptible to microbial contamination and once again confirms that this solvent
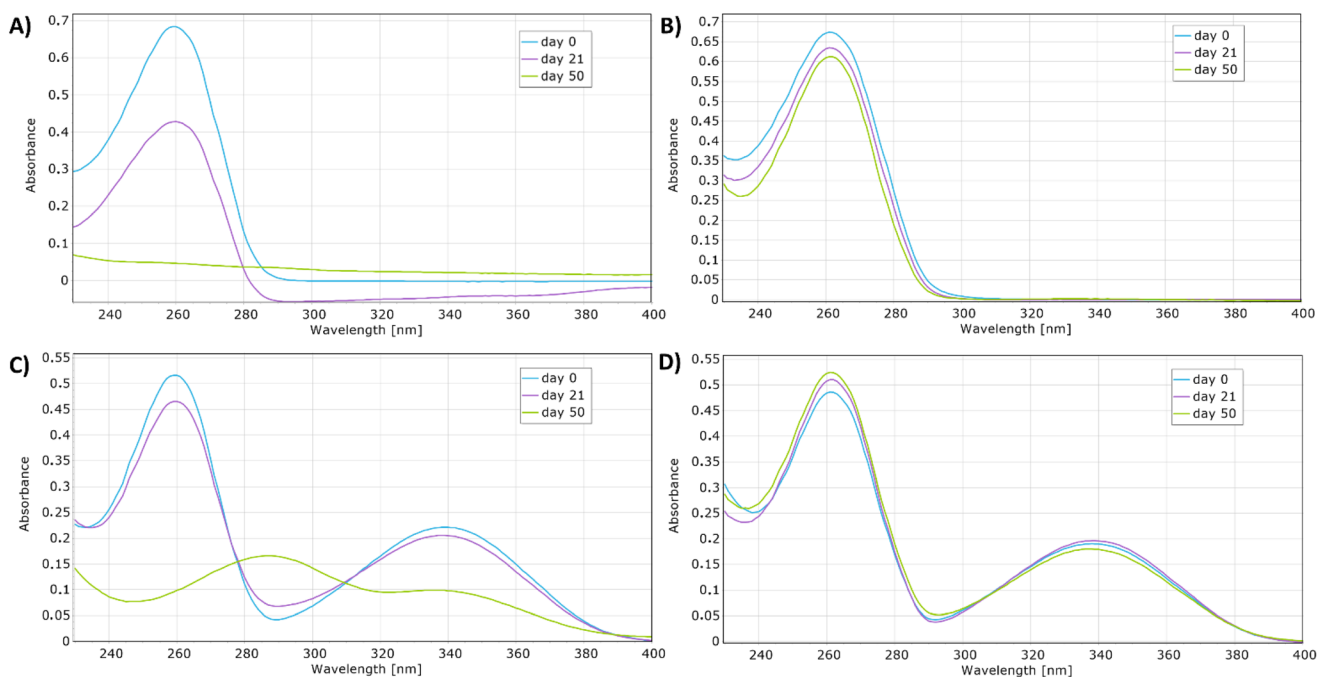
Fig. 5 Changes in absorption spectra of NAD coenzyme [0.03 mg mL^{-1}] after 0, 21, and 50-day incubation period in the best DES and buffer at room temperature. (A) NAD$^+$ in Tris–HCl buffer, (B) NAD$^+$ in ChCl:U$_{10\%}$, (C) NADH in Tris buffer, (D) NADH in ChCl:U$_{10\%}$.

could be used for the preparation of stable solutions of both NAD^+ and NADH.

The potential of ChCl:U for preparation of stable working NAD solutions

Encouraged by minimal deviations in the absorption spectrum of NAD coenzyme during prolonged incubation in ChCl:U (with all water contents), which are in direct correlation with DES excellent ability to stabilise the coenzyme,[28] we were wondering whether NAD solution in DES could be used as a working reagent solution for enzyme or substrate assays, or better to say, does the coenzyme retains its biological function (electron transfer in redox reactions) once it is dissolved or stored in DES. Therefore, to mimic the storage conditions that are being used for the preparation of working reagent solutions in practice, we conducted an additional set of experiments. Previously we demonstrated that the most favourable solvent for NAD^+ stabilisation is $ChCl:U_{80\%}$ (with the lowest absorption deviation, Δ_{260} = 6.17%), so we chose this DES for further examinations. These experiments included preparation of NAD^+ solution in $ChCl:U_{80\%}$ (0.05 g mL^{-1}) which was stored in dark at 4 °C for 50 days. At specific time intervals, the coenzyme functionality was tested by performing an alcohol dehydrogenase (ADH) activity assay in GlyPP buffer. As shown in Fig. 6, there is almost no change in enzyme volumetric activity (A_v) depending on NAD^+ incubation time in $ChCl:U_{80\%}$ and after the 50-day incubation period, A_v retained 88% of its initial value. Additionally, to see if DES itself interferes with the coenzyme's functionality, which would be seen as the change in enzyme activity, ADH activity was also measured by using NAD^+ working solution in buffer. The initial ADH activity assay showed that there is just a slight difference in enzyme volumetric activity when NAD^+ solution in DES or buffer is used for the assay (2.5 and 2.8 µmol min^{-1} cm^{-3}, respectively). That observation implies that conformational changes of the coenzyme (extended form) in DES, elucidated by MD simulations, do not influence NAD^+ ability to transport electrons during the enzyme-catalysed oxidoreductive reaction once transferred back into the buffer solution. This discovery directly implies that DES, specifically $ChCl:U_{80\%}$ could be used for the preparation of NAD^+ coenzyme working solutions stable for 50 days at 4 °C.

Moreover, the solution is also free from any kind of contamination and turbidity that could interfere with assays performed by using this working solution.

Future perspectives for enzymatic catalysis

The synergistic use of a DES and biocatalysis has been recognized as an efficient and sustainable way to produce various commercially significant products. Namely, as the number of structural combinations encompassed by DES is tremendous, in theory, it is possible to design an optimal DES for each specific enzymatic reaction system in terms of enzyme activity, selectivity and stability, as well of solvent compatibility with other reaction participants (*i.e.* substrates, co-substrates and coenzymes).[5] Thus, regardless of this research main objective, and that is to minimize NAD coenzyme degradation during storage and reagent preparation by the use of DES, the potential of using these solvents in enzymatic redox reaction requiring the NAD coenzyme is herein also discussed.

The ChCl:U, identified here as the best stabilising medium for the NAD coenzyme, is one of the first DES used for testing these solvents potential in enzymatic reactions. Namely, more than 15 years ago, Gorke *et al.*[63] demonstrated that high concentrations of urea (strong protein denaturant), paired with ChCl at a molar ratio 2 : 1, do not denature hydrolases. Moreover, later the Villeneuve group reported long-term stability of immobilised *C. antarctica* B at 50 °C in Ch:U where the loss of only 5% of the enzyme activity after 5 days of incubation was observed.[64] Several studies helped solving the enigma of how an enzyme can remain stable in a solvent with high urea content, and have shown that proteins exhibit excellent conformational stability in ChCl:U and that for this stabilizing effect high concentrations of both ChCl and U, at molar ratio 1 : 2 corresponding to a deep eutectic state, are vital.[65,66] To this day, it has been shown that other ChCl-based DES, those with polyols and sugars as HBD, stabilise versatile enzymes as well, usually at low water content. However, at such low water content, poor enzyme activities are often observed. By shifting water content in DES toward higher values, the activity of the enzymes usually increases and at optimal conditions reaches higher values than those in reference systems.[67–70]

Even though the influence of DES on enzymes has been closely examined, the behaviour of oxidoreductive enzymes in DES, especially those that are NAD dependent, is still not systematically explored. Ma *et al.*[71] studied ChCl-based DES with urea and polyols as alternative solvents for peroxygenase-catalysed reactions by using choline oxidase from *A. nicotianae* and the recombinant peroxygenase from *A. aegerita* as catalysts in the bienzymatic cascade for the selective oxyfunctionalisation of ethyl benzene or *cis*-β-methylstyrene. In case of the hydroxylation reaction, the highest product titers were observed in DES containing 75% of water, while in case of the epoxidation reaction 50% was found more favourable. Additionally, all
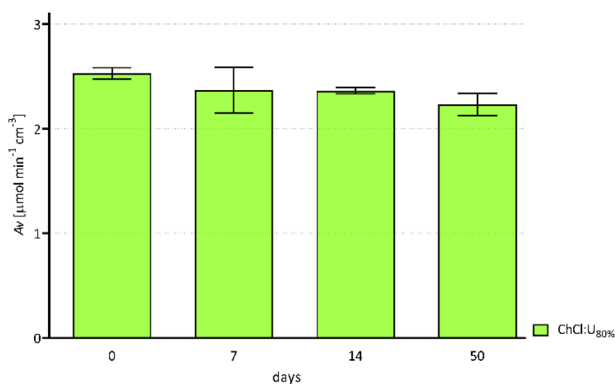

Fig. 6 Volumetric ADH activity depending on NAD^+ incubation time in $ChCl:U_{80\%}$.

DES–buffer systems tested (50 : 50) had a very pronounced stabilising effect on peroxygenase (much greater compared to referent buffer). Sun *et al.*[72] investigated the catalytic activity and thermal stability of NAD-dependent cytochrome P450 in a series of ChCl-based DES paired with urea and polyols (such as Gly, EG and PG) and observed that both the activity and the stability of the enzymes in DES were higher than that in buffer solution. For example, in ChCl:U at water contents above 60% improved enzyme catalytic activity and stability compared to reference organic solvent was observed (activity at lower water contents was not monitored). In our study we have shown that even at such high water content Ch:U stabilises NADH to a greater extent than the reference buffer, implying the potential of such ChCl:U–water mixtures for peroxygenase-catalysed reactions. According to the same study, the suitability of Ch:EG (yet another excellent candidate for stabilisation of the NAD coenzyme) at the same water shares as ChCl:U has been even more pronounced: a two-fold increase in the enzyme activity and residual activity after 5-day incubation in DES compared to buffer was observed. What is even more interesting, it has been shown that the ability of cytochrome P450 to recover from folding after heating to 80 °C and cooling down to room temperature in ChCl:U is concentration dependent: the less the water content, the stronger the protein's tertiary structure recovery ability. To be more precise, the highest protein tertiary structure recovery ability was observed in ChCl:U at water content of 25% (water concentration that corresponds to ChCl:U$_4$ that herein showed excellent stabilisation ability of both NAD coenzyme forms), which directly implies this medium's potential for long-term stabilisation of both the enzyme and the coenzyme. Based on these results, together with the results presented in this study, it could be expected that the use of ChCl:U-based working solutions (at low water content) containing both NAD coenzyme and enzyme could be extremely useful for the experimentalists working with the enzymes requiring NAD as coenzymes.

The use of whole cells overexpressing nicotinamide coenzyme dependent *Ralstonia* sp. ADH (RasADH) and horse liver ADH, overexpressed in *E. coli* in ChCl:Gly-aqueous media surprisingly revealed the maintenance of enzyme activity even at high DES contents of about 80%.[73] Additionally, low water content (up to 10%) drastically improved the stereoselectivity of RasADH for the bioreduction of propiophenone. The same DES, but with high glycerol loadings, was demonstrated as an excellent medium for the reduction of cinnamaldehyde catalysed by horse liver ADH (HLADH). In such DES the enzyme was highly active and stable, giving promising productivity.[68] To be more precise, a high HLADH half-life time peak was observed for ChCl:Gly at a water content of 40 vol% (higher than the half-life time observed in the aqueous buffer), which decreased at higher water contents. Even though we have shown that Ch:Gly at water content up to 35% is one of the least suitable DES for stabilisation of NAD coenzyme, these mixtures still showed improved coenzyme stabilisation ability compared to reference phosphate buffer commonly used for dehydrogenase-catalysed reactions, implying its potential as a storage medium.

Based on the results presented in this study, together with literature data on the activity and stability of the oxidoreductive enzymes in DES, it can be concluded that choline-based DES, at both low and high water contents, are promising solvents for enzyme-catalysed redox systems that require the NAD coenzyme, either as media for preparation of stable working solutions or as reaction media. It should be also mentioned that the pH value of a DES is not a detrimental factor influencing enzyme performance[5] and the ability to stabilise NAD coenzyme (as shown herein), thus cannot be used as a credible solvent parameter for finding the most suitable DES for a certain enzyme–coenzyme system. This practically means that for every reaction or substrate/coenzyme there is an optimal DES composition (HBD, HBA, water) which cannot be easily predicted and thus has to be systematically studied.

Conclusions

Choline-based DES with urea and ethylene glycol were identified as stabilisers of both reduced and oxidised NAD coenzyme forms. Computational analysis revealed that both coenzymes change their conformational preference and solvation environment in DES, whose components dominate in their tendency to solvate NAD$^+$ and NADH relative to water. The obtained insight showed that observed stability trends come as a result of an interplay between the component nucleophilicity, responsible for the cleavage of the phosphodiester P–O bond, and its basicity, determining the feasibility to undergo the nicotinamide–ribosyl N–C bond breaking, the latter being the prevailing degradation route especially for NAD$^+$. With this in mind, computations identified urea as the component which most optimally combines all three features, thereby allowing prolonged NAD stability in DES solutions where it is present.

ChCl:U showed the excellent capability to stabilise the NAD coenzyme during its incubation up to 50 days at 4 °C while preserving the coenzyme's biological functionality (electron transfer in reactions). Additionally, coenzyme solutions in ChCl:U were free of contamination and turbidity in the same period of time. All these facts pointed out the possibilities of using ChCl:U as NAD liquid storage medium, *i.e.* a working solution and assay reagent. Given that choline-based DES have been shown as an excellent medium for various NADH dependent dehydrogenases-catalysed reactions (in terms of enzyme activity and stability), presented results also imply that these DES should be considered as a solvent for complex redox reactions that require functionality and stability of both the enzyme and the coenzyme.

Abbreviations

DES	Deep eutectic solvents
HBA	Hydrogen bond acceptor
HBD	Hydrogen bond donor
MD	Molecular dynamics

B	Betaine
ChCl	Choline chloride
EG	Ethylene glycol
Gly	Glycerol
Gly–NaOH	Glycine–sodium hydroxide buffer
GlyPP	Glycine phosphate buffer
PBS	Phosphate-buffered saline
PG	Propylene glycol
U	Urea

Conflicts of interest

There are no conflicts to declare.

Acknowledgements

References

1 V. Hessel, N. N. Tran, M. R. Asrami, Q. D. Tran, N. V. D. Long, M. Escribà-Gelonch, J. O. Tejada, S. Linke and K. Sundmacher, *Green Chem.*, 2022, **24**, 410–437.

2 A. Paiva, R. Craveiro, I. Aroso, M. Martins, R. L. Reis and A. R. C. Duarte, *ACS Sustainable Chem. Eng.*, 2014, **2**, 1063–1071.

3 Y. Liu, J. B. Friesen, J. B. McAlpine, D. C. Lankin, S. N. Chen and G. F. Pauli, *J. Nat. Prod.*, 2018, **81**, 679–690.

4 M. Francisco, A. Van Den Bruinhorst and M. C. Kroon, *Angew. Chem., Int. Ed.*, 2013, **52**, 3074–3085.

5 M. Panić, M. Cvjetko Bubalo and I. Radojčić Redovniković, *J. Chem. Technol. Biotechnol.*, 2021, **96**, 14–30.

6 J. A. Kist, H. Zhao, K. R. Mitchell-Koch and G. A. Baker, *J. Mater. Chem. B*, 2021, **9**, 536–566.

7 D. Mondal, M. Sharma, C. Mukesh, V. Gupta and K. Prasad, *Chem. Commun.*, 2013, **49**, 9606–9608.

8 K. Bhakuni, N. Yadav and P. Venkatesu, *Phys. Chem. Chem. Phys.*, 2020, **22**, 24410–24422.

9 M. S. Lee, K. Lee, M. W. Nam, K. M. Jeong, J. E. Lee, N. W. Kim, Y. Yin, S. Y. Lim, D. E. Yoo, J. Lee and J. H. Jeong, *J. Ind. Eng. Chem.*, 2018, **65**, 343–348.

10 B. P. Wu, Q. Wen, H. Xu and Z. Yang, *J. Mol. Catal. B: Enzym.*, 2014, **101**, 101–107.

11 F. Xu, J. J. Kulys, K. Duke, K. Li, K. Krikstopaitis, H. J. W. Deussen, E. Abbate, V. Galinyte and P. Schneider, *Appl. Environ. Microbiol.*, 2000, **66**, 2052–2056.

12 M. Cvjetko Bubalo, A. Jurinjak Tušek, M. Vinković, K. Radošević, V. Gaurina Srček and I. Radojčić Redovniković, *J. Mol. Catal. B: Enzym.*, 2015, **122**, 188–198.

13 E. Su and A. M. Klibanov, *Appl. Biochem. Biotechnol.*, 2015, **177**, 753–758.

14 M. Ruesgas-Ramón, M. C. Figueroa-Espinoza and E. Durand, *J. Agric. Food Chem.*, 2017, **65**, 3591–3601.

15 Z. Wei, X. Qi, T. Li, M. Luo, W. Wang, Y. Zu and Y. Fu, *Sep. Purif. Technol.*, 2015, **149**, 237–244.

16 J. B. Barbieri, C. Goltz, F. Batistão Cavalheiro, A. Theodoro Toci, L. Igarashi-Mafra and M. R. Mafra, *Ind. Crops Prod.*, 2020, **144**, 112049.

17 M. Panić, V. Gunjević, G. Cravotto and I. Radojčić Redovniković, *Food Chem.*, 2019, **300**, 125185.

18 X. Peng, M.-H. Duan, X.-H. Yao, Y.-H. Zhang, C.-J. Zhao, Y.-G. Zu and Y.-J. Fu, *Sep. Purif. Technol.*, 2016, **157**, 249–257.

19 C. Lu, J. Cao, N. Wang and E. Su, *Med. Chem. Commun.*, 2016, **7**, 955–959.

20 Y. Zhang, C. Du, Y. Cong, Y. Xue, B. Qiao, T. Ye and M. Wang, *J. Chem. Eng. Data*, 2019, **64**, 5748–5754.

21 L. Rajman, K. Chwalek and D. A. Sinclair, *Cell Metab.*, 2018, **27**, 529.

22 T. Knaus, C. E. Paul, C. W. Levy, S. de Vries, F. G. Mutti, F. Hollmann and N. S. Scrutton, *J. Am. Chem. Soc.*, 2016, **138**, 1033–1039.

23 H. Wu, C. Tian, X. Song, C. Liu, D. Yang and Z. Jiang, *Green Chem.*, 2013, **15**, 1773–1789.

24 P. L. Hentall, N. Flowers and T. D. H. Bugg, *Chem. Commun.*, 2001, **1**, 2098–2099.

25 I. Zachos, C. Nowak and V. Sieber, *Curr. Opin. Chem. Biol.*, 2019, **49**, 59–66.

26 Z. Zhang, B. Xu, J. Luo, N. Von Solms, H. He, Y. Zhang, M. Pinelo and S. Zhang, *Catalysts*, 2018, **8**, 304.

27 J. T. Wu, L. H. Wu and J. A. Knight, *Clin. Chem.*, 1986, **32**, 314.

28 S. A. Margolis, B. F. Howell and R. Schaffer, *Clin. Chem.*, 1976, **22**, 1322–1329.

29 A. Vrsalović Presečki, K. Makovšek and Đ. Vasić-Rački, *Appl. Biochem. Biotechnol.*, 2012, **167**, 595–611.

30 L. Hok and R. Vianello, *Int. J. Mol. Sci.*, 2021, **22**, 1–16.

31 L. Ptiček, L. Hok, P. Grbčić, F. Topić, M. Cetina, K. Rissanen, S. K. Pavelić, R. Vianello and L. Racané, *Org. Biomol. Chem.*, 2021, **19**, 2784–2793.

32 N. Pantalon Juraj, G. I. Miletić, B. Perić, Z. Popović, N. Smrečki, R. Vianello and S. I. Kirin, *Inorg. Chem.*, 2019, **58**, 16445–16457.

33 L. Hok, J. Mavri and R. Vianello, *Molecules*, 2020, **25**, 6017.

34 T. Tandarić and R. Vianello, *ACS Chem. Neurosci.*, 2019, **10**, 3532–3542.

35 E. Mehić, L. Hok, Q. Wang, I. Dokli, M. S. Miklenić, Z. F. Blažević, L. Tang, R. Vianello and M. M. Elenkov, *Adv. Synth. Catal.*, 2022, **364**, 2576–2588.

36 J. M. Herbert, *Wiley Interdiscip. Rev.: Comput. Mol. Sci.*, 2021, **11**, e1519.

37 S. Ringe, N. G. Hörmann, H. Oberhofer and K. Reuter, *Chem. Rev.*, 2021, **122**, 10777–10820.

38 C. Gertig, K. Leonhard and A. Bardow, *Curr. Opin. Chem. Eng.*, 2020, **27**, 89–97.

39 M. J. Frisch, G. W. Trucks, H. B. Schlegel, G. E. Scuseria, M. A. Robb, J. R. Cheeseman, G. Scalmani, V. Barone, G. A. Petersson, H. Nakatsuji, X. Li, M. Caricato, A. V. Marenich, J. Bloino, B. G. Janesko, R. Gomperts, B. Mennucci, H. P. Hratchian, J. V. Ortiz, A. F. Izmaylov, J. L. Sonnenberg, D. Williams-Young, F. Ding, F. Lipparini, F. Egidi, J. Goings, B. Peng, A. Petrone, T. Henderson, D. Ranasinghe, V. G. Zakrzewski, J. Gao, N. Rega, G. Zheng, W. Liang, M. Hada, M. Ehara, K. Toyota, R. Fukuda, J. Hasegawa, M. Ishida, T. Nakajima, Y. Honda, O. Kitao, H. Nakai, T. Vreven, K. Throssell, J. A. Montgomery Jr., J. E. Peralta, F. Ogliaro, M. J. Bearpark, J. J. Heyd, E. N. Brothers, K. N. Kudin, V. N. Staroverov, T. A. Keith, R. Kobayashi, J. Normand, K. Raghavachari, A. P. Rendell, J. C. Burant, S. S. Iyengar, J. Tomasi, M. Cossi, J. M. Millam, M. Klene, C. Adamo, R. Cammi, J. W. Ochterski, R. L. Martin, K. Morokuma, O. Farkas, J. B. Foresman and D. J. Fox, *Gaussian 16 (Revision C.01)*, Gaussian Inc., Wallingford CT, 2016.

40 D. A. Case, R. C. Walker, T. E. Cheatham, C. Simmerling, A. Roitberg, K. M. Merz, R. Luo, T. Darden, J. Wang, R. E. Duke, D. R. Roe, S. LeGrand, J. Swails, D. Cerutti, G. Monard, C. Sagui, J. Kaus, R. Betz, B. Madej, C. Lin, D. Mermelstein, P. Li, A. Onufriev, S. Izadi, R. M. Wolf, X. Wu, A. W. Götz, H. Gohlke, N. Homeyer, W. M. Botello-Smith, L. Xiao, T. Luchko, T. Giese, T. Lee, H. T. Nguyen, H. Nguyen, P. Janowski, I. Omelyan, A. Kovalenko and P. A. Kollman, *Amber 2016*, University of California, San Francisco, 2016.

41 T. Darden, D. York and L. Pedersen, *J. Chem. Phys.*, 1993, **98**, 10089–10092.

42 M. Ester, H.-P. Kriegel, J. Sander and X. Xu, *Second Int. Conf. Knowl. Discov. Data Min*, 1996, pp. 226–231.

43 M. M. Aboelnga and S. D. Wetmore, *J. Am. Chem. Soc.*, 2019, **141**, 8646–8656.

44 L. R. Rutledge and S. D. Wetmore, *J. Am. Chem. Soc.*, 2011, **133**, 16258–16269.

45 L. W. Chung, W. M. C. Sameera, R. Ramozzi, A. J. Page, M. Hatanaka, G. P. Petrova, T. V. Harris, X. Li, Z. Ke, F. Liu, H. B. Li, L. Ding and K. Morokuma, *Chem. Rev.*, 2015, **115**, 5678–5796.

46 Z. Yang, in *Deep Eutectic Solvents: Synthesis, Properties, and Applications*, ed. D. J. Ramón and G. Guillena, John Wiley & Sons, Ltd, 1st edn, 2019, pp. 43–60.

47 L. Cicco, G. Dilauro, F. M. Perna, P. Vitale and V. Capriati, *Org. Biomol. Chem.*, 2021, **19**, 2558–2577.

48 L. Rover, J. C. B. Fernandes, G. D. O. Neto, L. T. Kubota, E. Katekawa and S. H. P. Serrano, *Anal. Biochem.*, 1998, **260**, 50–55.

49 S. G. A. Alivisatos, F. Ungar and G. Abraham, *Nature*, 1964, **203**, 973–975.

50 S. Tshepelevitsh, A. Kütt, M. Lõkov, I. Kaljurand, J. Saame, A. Heering, P. G. Plieger, R. Vianello and I. Leito, *Eur. J. Org. Chem.*, 2019, 6735–6748.

51 N. J. Oppenheimer, *Mol. Cell. Biochem.*, 1994, **138**, 245–251.

52 J. F. Biellmann, C. Lapinte, E. Haid and G. Weimann, *Biochemistry*, 1979, **18**, 1212–1217.

53 U. Eisner and J. Kuthan, *Chem. Rev.*, 1972, **72**, 1–42.

54 G. K. Schroeder, C. Lad, P. Wyman, N. H. Williams and R. Wolfenden, *Proc. Natl. Acad. Sci. U. S. A.*, 2006, **103**, 4052–4055.

55 J. G. Zalatan and D. Herschlag, *J. Am. Chem. Soc.*, 2006, **128**, 1293–1303.

56 R. Salvio and A. Casnati, *J. Org. Chem.*, 2017, **82**, 10461–10469.

57 R. Wolfenden, C. Ridgway and G. Young, *J. Am. Chem. Soc.*, 1998, **120**, 833–834.

58 M. T. D. Campbell, D. S. Jones, G. P. Andrews and S. Li, *Food Nutr. Res.*, 2019, **63**, 3419.

59 R. W. Johnson, T. M. Marschner and N. J. Oppenheimer, *J. Am. Chem. Soc.*, 1988, **110**, 2257–2263.

60 K. A. Rising and V. L. Schramm, *J. Am. Chem. Soc.*, 1997, **119**, 27–37.

61 C. E. Newall and A. M. Eastham, *Can. J. Chem.*, 1961, **39**, 1752–1756.

62 I. B. Blagoeva, I. G. Pojarlieff, D. T. Tashev and A. J. Kirby, *J. Chem. Soc., Perkin Trans. 2*, 1989, 347–353.

63 J. T. Gorke, F. Srienc and R. J. Kazlauskas, *Chem. Commun.*, 2008, 1235–1237.

64 E. Durand, J. Lecomte, B. Baréa, G. Piombo, E. Dubreucq and P. Villeneuve, *Process Biochem.*, 2012, **47**, 2081–2089.

65 S. Sarkar, S. Ghosh and R. Chakrabarti, *RSC Adv.*, 2017, **7**, 52888–52906.

66 H. Monhemi, M. R. Housaindokht, A. A. Moosavi-Movahedi and M. R. Bozorgmehr, *Phys. Chem. Chem. Phys.*, 2014, **16**, 14882–14893.

67 Y. Dai, J. van Spronsen, G. J. Witkamp, R. Verpoorte and Y. H. Choi, *Anal. Chim. Acta*, 2013, **766**, 61–68.

68 J. P. Bittner, N. Zhang, L. Huang, P. Domínguez De María, S. Jakobtorweihen and S. Kara, *Green Chem.*, 2022, **24**, 1120–1131.

69 M. Panić, M. Radović, I. Maros, A. Jurinjak Tušek, M. Cvjetko Bubalo and I. Radojčić Redovniković, *Process Biochem.*, 2021, **102**, 1–9.

70 M. Panić, M. Andlar, M. Tišma, T. Rezić, D. Šibalić, M. Cvjetko Bubalo and I. Radojčić Redovniković, *Waste Manag.*, 2020, **120**, 340–350.

71 Y. Ma, Y. Li, S. Ali, P. Li, W. Zhang, M. C. R. Rauch, S. J. P. Willot, D. Ribitsch, Y. H. Choi, M. Alcalde, F. Hollmann and Y. Wang, *ChemCatChem*, 2020, **12**, 989–994.

72 H. Sun, R. Xin, D. Qu and F. Yao, *J. Biotechnol.*, 2020, **323**, 264–273.

73 C. R. Müller, I. Lavandera, V. Gotor-Fernández and P. Domínguezdemaría, *ChemCatChem*, 2015, **7**, 2654–2659.